

# Electromagnetic Transient Simulation of Large Power Networks with Modelica

Alireza Masoom<sup>1</sup> Jean Mahseredjian<sup>1</sup> Tarek Ould-Bachir<sup>2</sup> Adrien Guironnet<sup>3</sup>

<sup>1</sup>Department of Electrical Engineering, Polytechnique Montreal, Canada,  
{alireza.masoom, jean.mahseredjian}@polymtl.ca

<sup>2</sup>Department of Computer Engineering, Polytechnique Montreal, Canada,  
tarek.ould-bachir@polymtl.ca

<sup>3</sup>Réseau de Transport d'Électricité, France,  
adrien.guironnet@rte-france.com

## Abstract

This paper presents the simulation of electromagnetic transients (EMTs) with Modelica. The advantages and disadvantages are discussed. Simulation performance and accuracy are analyzed through the IEEE 118-bus benchmark which includes EMT-detailed models with nonlinearities. The domain-specific simulator EMTP is used for validations and comparisons.

*Keywords: Modelica, Equation-based Modeling, Acausal modeling, Electromagnetic transients, EMT, Synchronous machines, Large scale, Nonlinearity, IEEE 118-bus grid.*

## 1 Introduction

Power system simulations are mainly categorized into phasor-domain and time-domain. In phasor-domain analysis, voltages and currents are computed as phasors varying in time. The electrical network is solved in steady-state and at the fundamental frequency. Power generation sources, such as synchronous machines, are solved with their differential equations in time-domain and interfaced with network equations using phasor equivalents. The phasor-domain approach is suitable for electromechanical transients, load flow, and short-circuit studies in very large-scale grids and can be applied to any linear system but becomes less accurate with the presence of power electronics-based equipment e.g., FACTS and HVDC since this technique cannot represent the faster transients. Its main advantage remains computational speed for studying lower frequency transients, but harmonics and nonlinear models are ignored.

In the time-domain simulation approach, the network and all integrated components are solved in time-domain with detailed differential equations. Harmonics and nonlinearities are modeled accurately. The solution may include lower frequency interactions, as well as very high-frequency transients. The time-domain approach allows to solve networks for electromagnetic transients and is tagged as the EMT-type solution.

Various specialized EMT-type simulation tools (Mahseredjian 2009) are currently available and well adapted for studying various power system phenomena, including transformer saturation effects, lightning and

switching transients, and integration of inverter-based resources. Power electronics-based components can be simulated very accurately.

The EMTP (Mahseredjian, et al. 2007) software used in this paper is widely used for the EMT simulations. The cornerstone of this software is the discretization of component models using the well-known companion circuit approach. The A-stable trapezoidal and Backward-Euler numerical integration methods are employed for the discretization. The latter is used at discontinuity points to avoid numerical oscillations (Sana, Mahseredjian, et al. 1995). In EMTP, the companion circuits of components are interconnected (to respect Kirchhoff's first law) through a sparse matrix solver using the Modified Augmented Nodal Analysis (Mahseredjian, Dennetière, et al. 2007) formulation.

In power system modeling, Modelica has been first considered for phasor-domain simulations. iTesla Power Systems Library (iPSL) (Vanfretti et al. 2016) is a comprehensive Modelica package that was generated through the iTesla project (Lemaitre 2014) for unified modeling and for facilitating network model exchanges amongst transmission system operators. PowerGrids (Bartolini et al. 2019) and ObjectStab (Larsson 2004) are other advanced libraries developed for electromechanical and stability analyses, respectively.

Modelica (Fritzson 2014) is an *equation-based* language that relies on the description of a system by differential-algebraic equations. The EMT behavior of electrical components can be modeled by their differential equations. The language emphasizes the *acausal* approach based on *declarative* modeling where the model and solver are decoupled. It significantly improves model development process and model readability.

The first attempt to develop a Modelica-based *EMT-detailed* simulator was reported in (Masoom et al. 2020), where transmission lines incorporating the constant parameter and wideband (Kocar Mahseredjian 2016) models were introduced and validated. An EMT-detailed library was developed and validated using the IEEE 39-bus network.

A challenging problem with Modelica is computational speed (including compilation and simulation time). Some

solutions are based on numerical optimizations, e.g., Jacobian optimization (Kofman, Fernández, and Marzorati 2021) and simulation in DAE mode (Braun et al. 2017; Henningson 2019). An open-source solution (called Dynaωo) is specifically designed for power system simulations in phasor-domain (Guironnet et al. 2018). Dynaωo approach is based on hybrid coding with Modelica and C++ and demonstrates competitive performance compared to the specific domain packages (Guironnet et al. 2018). This approach was used for EMT simulations in (Masoom et al. 2021) as well. Even though it delivers better performance compared to the pure Modelica tools, there is still a significant gap in comparison with EMTP.

The IEEE 118-bus benchmark contains the following models: synchronous generators (including magnetic saturation model) with controls, transformers, transmission lines, nonlinear inductances, and nonlinear surge arresters. The basic models, such as resistance, inductance, and advanced models, that is, various models of transmission line, loads, saturable transformers, synchronous machine (without saturation), machine controls, etc. were already presented in previous papers (Masoom et al. 2020; Masoom et al. 2021). This paper focuses on the synchronous machine model with saturation and the nonlinear arrester and comparison of simulation efficiency in Modelica.

The paper is organized as follows. Two selected models, namely the synchronous machine and nonlinear arrester are developed using Modelica in Section 2. The numerical results for the IEEE 118-bus system are provided in Section 3.

## 2 Modelica Model Implementation

In this Section, two nonlinear models are presented and discussed in more detail. The models have been developed based on EMTP mathematical representations.

### 2.1 Synchronous Machine Model with Magnetic Saturation

The details required to model Synchronous Machine (SM) depend on the type of transient study. Saturation effects in SM are important for EMT analysis. Assuming the SM is modeled by two damping windings on the  $q$ -axis (denoted by  $kq1$ ,  $kq2$ ) and one damper winding ( $kd$ ) and one field winding ( $fd$ ) on the  $d$ -axis, (1)-(6) provide the flux-based equations of SM in *state-variable form*.

$$\mathbf{v}_{dq0} = \mathbf{P}(\theta)\mathbf{v}_{abc}/V_{stator,base} \quad (1)$$

$$p\boldsymbol{\Psi} = \omega_b(\mathbf{A}\boldsymbol{\Psi} + \mathbf{u}) \quad (2)$$

$$\mathbf{A} = -(\mathbf{R}\mathbf{L}^{-1} + \mathbf{W}) \quad (3)$$

$$\mathbf{i} = \mathbf{L}^{-1}\boldsymbol{\Psi} \quad (4)$$

$$\mathbf{i}_{abc} = \mathbf{P}^{-1}(\theta)\mathbf{i}_{dq0} \quad (5)$$

$$\mathbf{i}_{abc,actual} = \mathbf{i}_{abc} \cdot I_{stator,base} \quad (6)$$

where:

$$\mathbf{u} = [v_q, v_d, v_{fd}, 0, 0, 0]^T \quad (7)$$

$$\boldsymbol{\Psi} = [\Psi_q, \Psi_d, \Psi_{fd}, \Psi_{kd}, \Psi_{kq1}, \Psi_{kq2}]^T \quad (8)$$

$$\mathbf{i} = [i_q, i_d, i_{fd}, i_{kd}, i_{kq1}, i_{kq2}]^T \quad (9)$$

$$\mathbf{i}_{dq0} = [-i_q, -i_d, 0]^T \quad (10)$$

$$\mathbf{R} = \text{diag}(R_a, R_a, R_{fd}, R_{kd}, R_{kq1}, R_{kq2}) \quad (11)$$

In the above equations, the operator  $p$  is  $\frac{d}{dt}$ , the vector  $\mathbf{v}_{abc}$  is the terminal voltage,  $\mathbf{v}_{dq0}$  is the voltage in  $dq$  frame,  $\omega_b$  is the base angular velocity,  $\mathbf{P}(\theta)$  is the Park's transformation, vectors  $\mathbf{u}$ ,  $\mathbf{i}$ , and  $\boldsymbol{\Psi}$  denote the stator and rotor voltages, currents, and flux linkages in the  $dq$  frame and  $\mathbf{i}_{abc}$  is the stator current.  $\mathbf{W}_{6 \times 6}$  is the rotor speed-dependent matrix; all elements are zero except  $w[1,2] = \omega_r$  and  $w[2,1] = -\omega_r$ ,  $\mathbf{L}_{6 \times 6}$  is the symmetrical matrix of inductances in the rotor reference frame,  $\mathbf{R}_{6 \times 6}$  is the stator and rotor resistance matrix.

The details of saturation effects modeling in the  $dq$  axes are explained in (Karaagac et al. 2011). In magnetic saturation modeling, the following assumptions are made: (1) The leakage flux saturation and cross saturation are ignored. It means only magnetizing inductances,  $L_{md}$  and  $L_{mq}$  are saturable. (2) Saturation is determined by the air-gap flux linkage. (3) The sinusoidal distribution of the magnetic field over the face of the pole is unaffected by saturation.

Since the saturation relationship between the total air-gap flux,  $\Psi_T$ , and the magnetomotive force under loaded conditions is assumed to be the same as at no-load conditions, therefore magnetic saturation of stator and rotor iron can be modeled by the *no-load saturation curve* which is characterized by a *piecewise linear* graph (Karaagac et al. 2017).

Consequently, the mathematical model of saturation is introduced by:

$$\Psi_T = f(\Psi_{T,us}) = f\left(\sqrt{\Psi_{md,us}^2 + \Psi_{mq,us}^2}\right) \quad (12)$$

$$\begin{aligned} \Psi_{md,us} &= L_{md,us} i_{md} \\ i_{md} &= i_d + i_{fd} + i_{kd} \end{aligned} \quad (13)$$

$$\begin{aligned} \Psi_{mq,us} &= L_{mq,us} i_{mq} \\ i_{mq} &= i_q + i_{kq1} + i_{kq2} \end{aligned} \quad (14)$$

where  $\Psi_{T,us}$  is the total unsaturated air-gap flux,  $\Psi_{md,us}$  and  $\Psi_{mq,us}$  are the unsaturated magnetizing flux linkages,  $L_{md,us}$  and  $L_{mq,us}$  are the unsaturated magnetizing inductances, and  $i_{md}$  and  $i_{mq}$  are the magnetizing currents; each on the  $dq$  axis, respectively. Throughout the paper, the subscript *sat* and *us* mean saturated and unsaturated, respectively.

The value of saturated magnetizing flux linkages on the  $dq$  axis ( $\Psi_{md,sat}$  and  $\Psi_{mq,sat}$ ) can be corrected by a ratio of corresponding unsaturated values as illustrated in Figure 1.a. In EMTP, the magnetic saturation is represented by a *piecewise linear* curve as sketched in Figure 1.b. For the  $j^{\text{th}}$  operating segment,  $\Psi_T$  is given by:

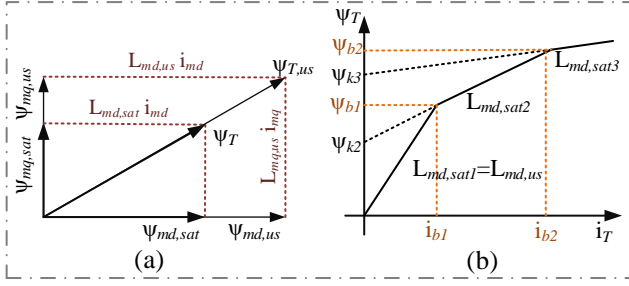


**Figure 1.** (a): Saturated and unsaturated magnetizing flux linkages in the  $dq$  axes of a synchronous machine. (b): Magnetic saturation characteristic (piecewise-linear approximation).

$$\Psi_T = \Psi_{kj} + b_j \Psi_{Tu} \quad (15)$$

$$= \Psi_{kj} + b_j L_{md,us} i_T$$

$$i_T = \sqrt{i_{md}^2 + \left(\frac{L_{mq,us}}{L_{md,us}}\right)^2 i_{mq}^2} \quad (16)$$

$$b_j = \frac{L_{md,satj}}{L_{md,us}} \quad (17)$$

where  $b_j$  is the saturation factor and  $\Psi_{kj}$  is the residual flux. The saturated values  $L_{md,sat}$  and  $L_{mq,sat}$  are computed as:

$$\begin{aligned} L_{md,sat} &= b_j L_{md,us} \\ L_{mq,sat} &= b_j L_{mq,us} \end{aligned} \quad (18)$$

For a *salient pole* machine, because of large airgap path along the  $q$ -axis, it is only required to correct the  $\Psi_{md}$ : thus:

$$\begin{aligned} L_{md,sat} &= b_j L_{md,us} \\ L_{mq,sat} &= L_{mq,us} \end{aligned} \quad (19)$$

Figure 2 demonstrates the solution procedure for the electrical equations of SM. In the case of no saturation, the relationship between field current ( $i_{fd}$ ) and terminal voltage ( $v_t$ ) is linear; therefore, the magnetizing inductances in (20) are constant ( $q_j = d_j = 1$ ). If saturation is selected, it is required to compute the magnetizing inductances at each time point; thus,  $\mathbf{L}$  is time-variant ( $q_j = d_j = b_j$  for round rotor and  $q_j = 0$ ,  $d_j = b_j$  for salient pole machine). This method results in implicit equations requiring an *iterative* solution.

The model discussed above has been implemented for the first time in Modelica. The model code is illustrated in Figure 3. The declaration of variables and the conversion of operational parameters to the standard ones are hidden to conserve space and only the equation section is demonstrated. The terminal voltages of SM are

$$\mathbf{L} = \begin{pmatrix} L_{ls} + q_j L_{mq,us} & 0 & 0 & 0 & q_j L_{mq,us} & q_j L_{mq,us} \\ 0 & L_{ls} + d_j L_{md,us} & d_j L_{md,us} & d_j L_{md,us} & 0 & 0 \\ 0 & d_j L_{md,us} & L_{lf} + d_j L_{md,us} & d_j L_{md,us} & 0 & 0 \\ 0 & d_j L_{md,us} & d_j L_{md,us} & L_{lk} + d_j L_{md,us} & 0 & 0 \\ q_j L_{mq,us} & 0 & 0 & 0 & L_{lkq1} + q_j L_{mq,us} & q_j L_{mq,us} \\ q_j L_{mq,us} & 0 & 0 & 0 & q_j L_{mq,us} & L_{lkq2} + q_j L_{mq,us} \end{pmatrix} \quad (20)$$

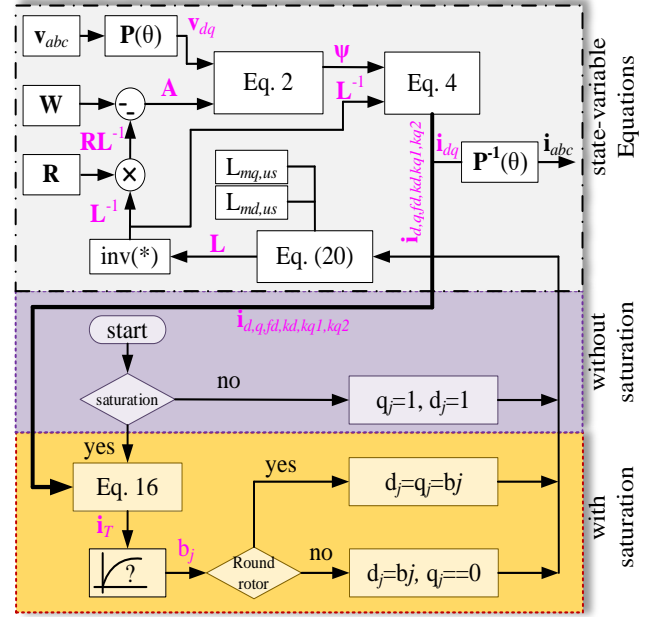


**Figure 2.** Solution procedure of synchronous machine with/without magnetic saturation in Modelica (Only electrical equations are demonstrated).

represented by  $Pk.pin[1].v$ ,  $Pk.pin[2].v$  and  $Pk.pin[3].v$  for the phases  $a$ ,  $b$  and  $c$ , respectively.  $P(\theta)$  represents a pre-defined function for the Park's transformation calculations.

Equation (2) is used as a differential equation for the implemented model; the state vector  $\Phi$  represents the flux linkages and the input vector  $\mathbf{u}$  the voltages. The system matrix  $\mathbf{A}$  is time-variant and computed as per (3).

The matrix of parameters for representation of saturation,  $\mathbf{SD}$ , is given by a 2-by- $n$  matrix, where  $n$  is the number of points taken from the no-load saturation curve. The first row of this matrix contains the values of field currents (physical value), while the second row contains values of corresponding terminal voltages (per unit).  $LinearInterplate(\mathbf{SD1PU}, \mathbf{SD2PU}, i_T)$  is a function to interpolate the  $i_T$  by the two vectors of field current ( $\mathbf{SD1PU}$ ) and voltage ( $\mathbf{SD2PU}$ ). These two vectors are calculated in the *non-reciprocal* per unit. The function returns the total flux ( $\Phi_{iT}$ ) and  $L_{mdsat}$  which the latter is used for calculation of coefficient  $b$  as per (17). The stator physical currents are represented by  $Pk.pin[1].i$ ,  $Pk.pin[2].i$  and  $Pk.pin[3].i$  for the phases,  $a$ ,  $b$  and  $c$ , respectively.

Other pieces of code represent the mechanical equations of SM which are not discussed in this paper.

```

model SM "Synchronous Machine 6 order including
saturation"
// Declaration of variables and parameters are hidden
due to space limitations.
equation
// Conversion of terminal voltage to pu
vabc = {Pk.pin[1].v, Pk.pin[2].v, Pk.pin[3].v} / Vsbase;
// Conversion from abc frame to dq0 frame
vdq0 = P(theta) * vabc;
// State space electrical equations
der(Phi) = Wb * (A * Phi + u);
A = -(R * inv(L) + W);
i = inv(L) * Phi;
// Implementation of magnetic saturation
imd = Ip[2] + Ip[3] + Ip[4]; //imd = id + ifD + ikd
imq = Ip[1] + Ip[5] + Ip[6]; //imq = iq + ikq1 + ikq2
iT = sqrt(imd^2 + (Lmqus/Lmdus)^2 * imq^2); Eq.(16)
(PhiT, Lmdsat) = LinearInterpolation(SD1pu, SD2pu, iT);
b = Lmdsat / Lmdus; Eq.(17)
if Saturation then
    if RoundRotor then
        q=b;
        d=b;
    else
        q=0;
        d=b;
    end if;
else
    q=1;
    d=1; Eq.(20)
end if;
Lq = Lls + q * Lmqus;
Ld = Lls + d * Lmdus;
Lffd = Lffd + d * Lmdus;
Lkdkd = Llkd + d * Lmdus;
Lkqlkq1 = Llkq1 + q * Lmqus;
Lkq2kq2 = Llkq2 + q * Lmqus;

L= [ Lq , 0 , 0 , 0 , q*Lmqus , q*Lmqus ;
    0 , Ld , d*Lmdus , d*Lmdus , 0 , 0 ;
    0 , d*Lmdus , Lffd , d*Lmdus , 0 , 0 ;
    0 , d*Lmdus , d*Lmdus , Lkdkd , 0 , 0 ;
    q*Lmqus , 0 , 0 , 0 , Lkqlkq1 , q*Lmqus ;
    q*Lmqus , 0 , 0 , 0 , q*Lmqus , Lkq2kq2 ];

// Conversion from dq0 to abc frame
iabc = inv(P(theta)) * idq0;
// Calculations of actual Terminal current
Pk.pin[1].i = -iabc[1] * Isbase;
Pk.pin[2].i = -iabc[2] * Isbase;
Pk.pin[3].i = -iabc[3] * Isbase;
// Mechanical equations
Te = Phi[2] * idq0[1] - Phi[1] * idq0[2];
Tnet = Tm - Te - D * dw;
Tm = Pm_pu / Wr;
der(dw) = Tnet * (1 / 2 / H);
Wr = 1 + dw;
der(d_theta) = dw * Wb;
theta = d_theta + Wb * time;
// where
// u = {Vq , Vd , Vfd , Vkd , Vkq1 , Vkq2 }
u = {vdq0[1], vdq0[2], vfd, 0, 0, 0};
// Phi = {Phiq , Phid , Phifd , Phikd , Phikq1, Phikq2 }
Phi = {Phi[1], Phi[2], Phi[3], Phi[4], Phi[5], Phi[6]};
// i = {iq , id , ifd , ikd , ikq1 , ikq2 }
i = {i[1], i[2], i[3], i[4], i[5], i[6]};
// Change of sign due to generating mode
idq0 = {-i[1], -i[2], 0};
W[6, 6] = [ 0 , Wr , 0 , 0 , 0 , 0 ;
    -Wr , 0 , 0 , 0 , 0 , 0 ;
    0 , 0 , 0 , 0 , 0 , 0 ;
    0 , 0 , 0 , 0 , 0 , 0 ;
    0 , 0 , 0 , 0 , 0 , 0 ;
    0 , 0 , 0 , 0 , 0 , 0 ];
R[6, 6] = diagonal({Rs, Rs, Rfd, Rkd, Rkq1, Rkq2});
end SM;
    
```

**Figure 3.** Implementation of synchronous machine model with magnetic saturation in Modelica. The saturation formulation is distinguished with the blue dashed frame.

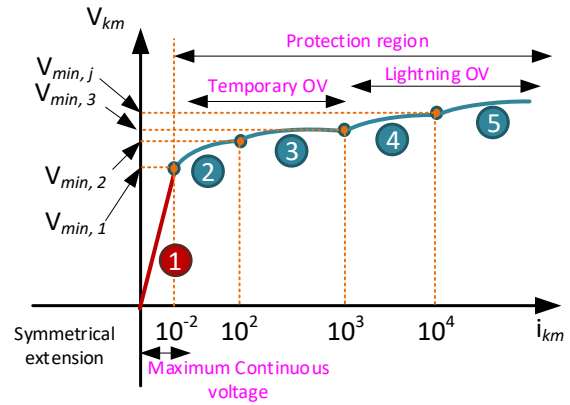


**Figure 4.** Voltage-current characteristic of ZnO surge arrester and operating regions.

## 2.2 Nonlinear Arrester Modeling

Surge arresters protect the insulation of equipment, e.g., transformers in electrical systems against overvoltage transients caused by lightning or switching surges. The voltage and current characteristic of a gapless metal-oxide surge arrester as illustrated in Figure 4 is a severely nonlinear resistor with an *infinite* slope in the normal operation region and an almost *horizontal* slope in the protection region (temporary and lightning overvoltages). In EMTP, the nonlinear resistance is represented by the following *power* function:

$$i_{km} = p_j \left( \frac{v_{km}}{V_{ref}} \right)^{q_j} \quad (21)$$

where  $i_{km}$  and  $v_{km}$  are arrester current and voltage,  $j$  is the segment number starting at the voltage  $V_{min,j}$ , multiplier  $p_j$  and exponent  $q_j$  are coefficients defined for each  $V_{min,j}$  and  $V_{ref}$  is the arrester reference voltage. A *linear* function is used for the first segment.

The technique for modeling a nonlinear resistance (arrester function) is like the one used for the nonlinear

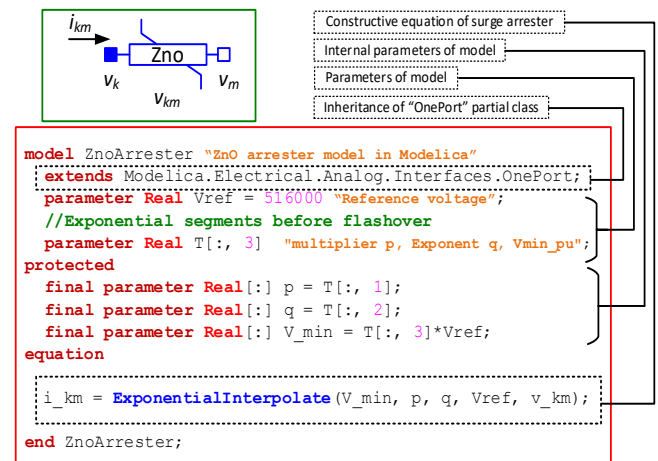


**Figure 5.** Implementation of the ZnO surge arrester model in Modelica environment.

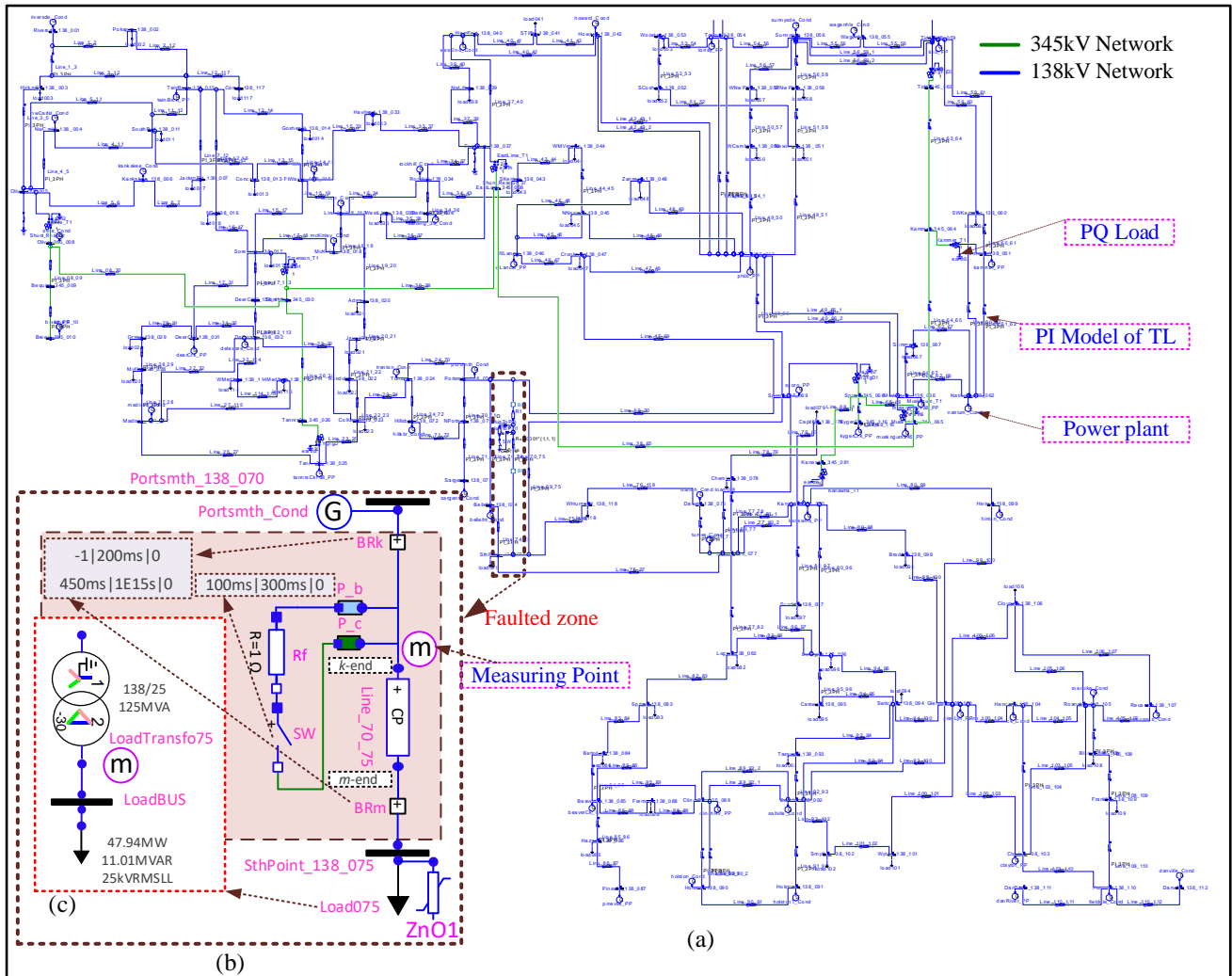


**Figure 6.** (a): IEEE 118-bus Network including 177 PI-section models of TL sketched using the Modelica GUI. (b): the faulty zone; a phase-*b*-to-phase-*c* fault at *k*-end of Line\_70\_75. The powerplant “Portsmth\_Cond” is selected for validation of SM with saturation in Case 2, Surge arrester ZnO1 is inserted in the circuit only for Case 3. (c): the sub-circuit of Load75 including a saturable transformer model and constant-impedance model of load.

inductance. Figure 5 illustrates the code for the implementation of the surge arrester. The parameters of  $p_j$ ,  $q_j$  and  $V_{min_j}$  are defined by  $n$ -by-3 matrix,  $\tau$ .

ExponentialInterpolate() is a function defined by the specific class function, where the operating voltage is searched for the appropriate segment,  $j$ . Then, the value of  $i_{km}$  is exponentially interpolated using (21). The properties of partial class OnePort are inherited to apply the appropriate equations of one-port devices.

As one can see, the implementation of the model is very straightforward, there is no limitation for connection of this model in series to current sources, or inductors. Solutions converge for very small time steps in the range of nanoseconds without any numerical errors (Masoom et al. 2021).

### 3 Model Verification and Validation

This section presents simulation results of the modified IEEE 118-bus benchmark (Haddadi, Mahseredjian, et al.

2018) which is used to validate the accuracy of the proposed models. The same test case is also simulated with EMTP.

Figure 6.a shows the schematic diagram of the IEEE 118-bus network sketched using the developed EMT library in Modelica. A user-friendly Graphical User Interface (GUI) with an illustrative icon is designed for each component model for entering the parameters and drawing networks easily. The physical connection of components is carried out by interconnecting the terminals of appropriate components.

The IEEE-118 bus circuit consists of 54 generating units with controls (a few power plants contain more than one SM; the total number of SMs is 69), 177 transmission lines (RL coupled), 9 three-winding grid transformers, 145 two-winding transformers (91 Yd1-connected load-serving transformers+ 54 generator transformers), and 91 three-phase loads. The voltage levels are 345kV transmission, 138kV sub-transmission, 25kV distribution, and {20, 15, 10.5} kV generation. The network includes



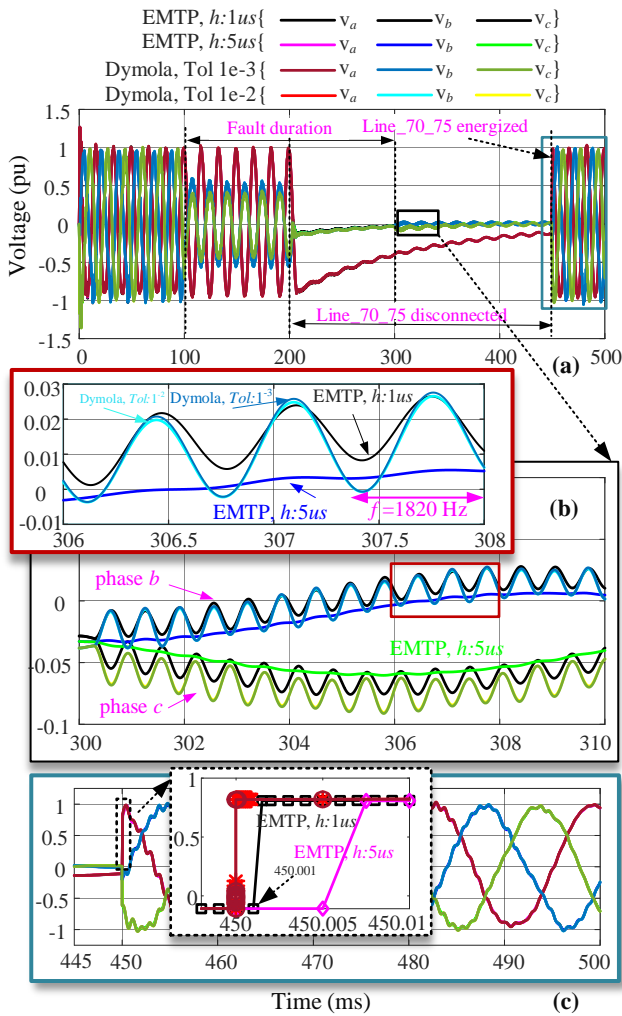


**Figure 7.** (a): Voltage waveforms of phases *a*, *b* and *c* at the *k*-end of Line\_70\_75; (b): comparison of results for the phases *b* and *c* for different solvers’ parameters. (c): voltage waveforms after re-energization of Line\_70\_75; the close-up at the instant of closing the breakers BRk and BRm.

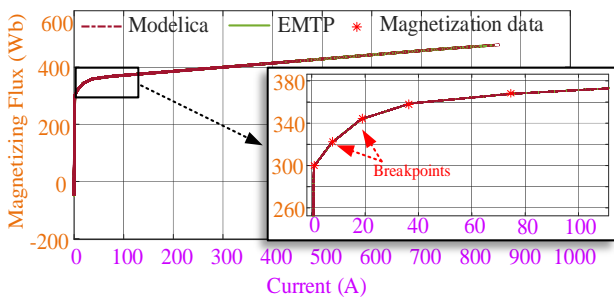


**Figure 8.** Current-Flux curve of magnetization branch in the LoadTransfo75 transformer; close-up of Modelica and EMTP solutions near to the knee-point.

519 nonlinear inductances and 1909 RLC elements. All SMs use a single-mass Wye-grounded model including the normalized saturation characteristics represented by 7 points. The SM control systems consist of exciter type ST1, steam turbine and governor type IIESGO, synchronous machine phasor and power system stabilizer

type PSS1A. The model of all three-phase transformers consists of three single-phase units. The nonlinear magnetization branch is placed on the high-voltage side. The model uses a piecewise linear current-flux curve defined by 8 points (in the positive part of the symmetric characteristic) to represent saturation. All loads are represented by a constant impedance model.

The transmission lines (TL) are modeled using pi-sections. The constant parameter line model with propagation delay is simulated slowly, owing to the very high computational cost of the Modelica built-in delay operator. Simulation of the network starts with zero initial states.

### 3.1 Case 1: Phase-to-Phase Fault Analysis

For creating a transient disturbance, (see Figure 6.b), a temporary phase-to-phase fault with a fault resistance of  $1 \Omega$  is applied on the phases ‘*b*’ and ‘*c*’ of “Line\_70\_75” at  $t = 100$  ms followed by the isolation of the line at  $t = 200$  ms (i.e. the breakers BRm and BRk open simultaneously after 6 cycles). The fault is cleared at  $t = 300$  ms, then the line is reconnected at  $t = 450$  ms.

Re-energizing the TL introduces high-frequency transient oscillations and allows to investigate the accuracy of transformer models in nonlinear regions.

For this purpose, the curve of flux versus current for LoadTransfo75 which is located near the faulty line is compared with EMTP as well.

Numerical tests are performed using the variable-step DASSL solver (Petzold 1982) in ODE mode with the tolerance of  $1e-3$  and the maximum integration order of 5 in Dymola 2021x. In EMTP, Trapezoidal/Backward Euler integrator with the step sizes of  $1 \mu s$  and  $5 \mu s$  is employed. The simulation time is 500 ms. The network model in Modelica contains 96308 acausal DAEs. The total number of network nodes and the size of the main system of equations in EMTP are 2533 and 3773, respectively.

Figure 7.a depicts the voltage waveforms of phases *a*, *b* and *c* at the *k*-end of Line\_70\_75 obtained by the two simulators with different precisions. An excellent agreement is observed between the results. Figure 7.b shows the simulation results for the phases *b* and *c* in the interval of [300, 310] ms, i.e., after the fault is removed. The results produced by Modelica models are almost identical to EMTP when step size is  $1 \mu s$  (black curve), whilst the high-frequency transient oscillations ( $f=1820$  Hz) are not captured by EMTP when  $\Delta t = 5 \mu s$  (blue curve). Figure 7.c depicts the curves of voltage after the re-energization of TL. The consistent results between Modelica and EMTP are observed in this period once more. The close-up view of the phase *a* voltage waveform at the instant of closing the breakers BRm and BRk shows that Modelica voltage waveform rises precisely at  $t = 450$  ms while in EMTP it goes up in the next time point. The close-up illustrates the discontinuity treatment discrepancies between the two simulators. This is an

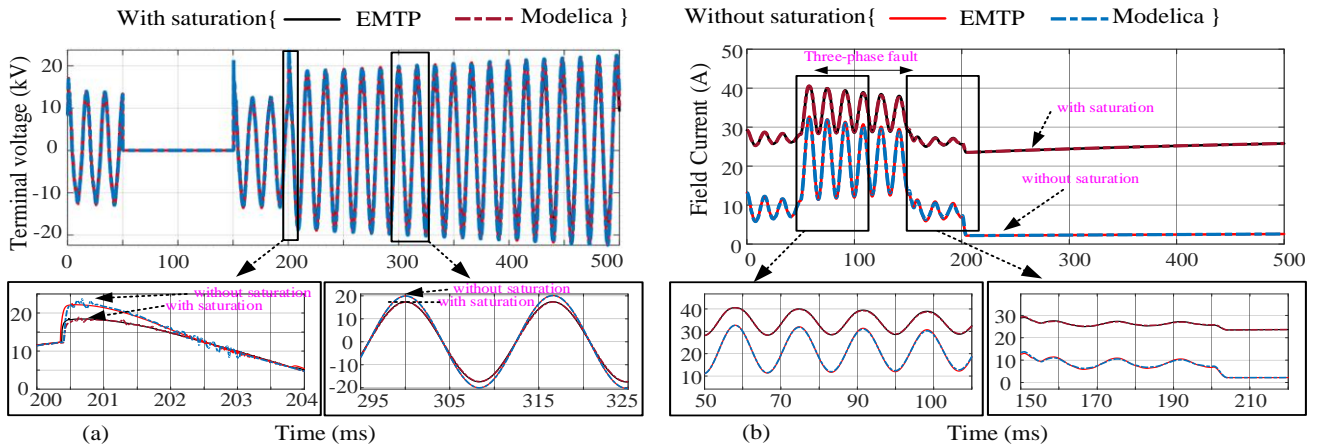


**Figure 9.** (a): Waveform of phase-*a* stator voltage of SM with and without saturation model; the close-up after load rejection. (b): field current with and without saturation model; the zoomed views during and after fault.

**Table 1.** Case 1: comparison of simulation performance.

Characteristics	Dymola		EMTP		
	DASSL		Trapezoidal/Backward Euler		
Tolerance	1e-3	1e-2			
$\Delta t_{MIN}$	0.115 fs	0.116 fs	$\Delta t: 1 \mu s$	$\Delta t: 5 \mu s$	$\Delta t: 10 \mu s$
$\Delta t_{MAX}$	5.79 $\mu s$	0.16 $\mu s$			
No result points	203035	335261	601757	154367	81 661
No accepted steps	203034	335260	Not applicable		
f-evaluations	415437	760052	Not applicable		
J-evaluations	7393	337458	Not applicable		
CPU time (s)	371.2	1510.6	110.1	44.2	23.5
CPU-time for 1 accepted steps	1.83 ms	4.49 ms	0.18 ms	0.28 ms	0.28 ms
Performance ratio	1	0.24	3.37	8.39	15.79

important issue for the simulation of circuits with high-frequency switching.

For validating the accuracy of nonlinear components, the magnetization branch curve of LoadTransfo75 (see Figure 6.c) is examined in Figure 8. Once again, the results obtained by the two models show an excellent agreement and transformer operating points (depicted by the red dashed line) move on the transformer current-flux characteristics (distinguished by the solid red line). The *iterative* solution allows reproducing the nonlinear function accurately in both tools.

The number of nonlinear components and control closed loops has a significant impact on the accuracy and speed of simulation. For example, simulation of the same network, that is IEEE 118-bus, jams in Simscape Electrical Specialized Power Systems (SPS) package (Simscape Electrical 2020) which is comparable to Modelica environment in some ways. This package is based on the *state-space* representation of the linear network in a loop with external current sources denoting the nonlinear components. In Modelica, nonlinear functions are solved *simultaneously* through *iterative* methods which gives the most accurate results.

Table 1 shows the data and run-times of simulations carried out in Dymola and EMTP. The CPU times are extracted from the average of 5-times “re-simulations”. In Dymola, simulation is accomplished with 203034 steps in

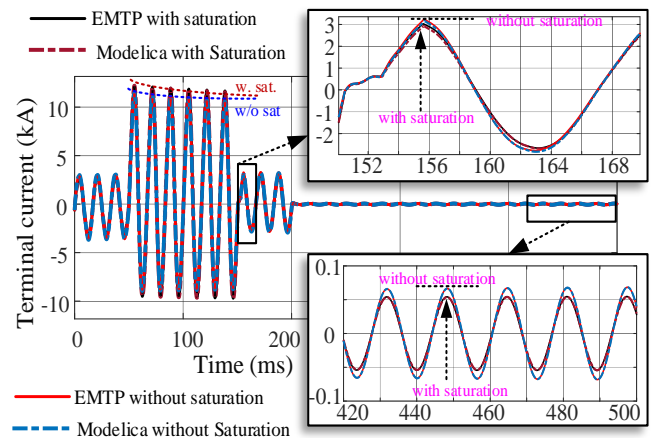


**Figure 10.** Phase-*a* stator current with and without saturation model; zoomed view after removing the fault and load rejection.

371.2 s, which yields 1.83 ms for each time step. EMTP outperforms Dymola with the ratio of 3.37:1 when the least error is favorite, i.e.,  $\Delta t = 1 \mu s$ .

Tolerance has a significant impact on the CPU time and the number of time steps for the DASSL since the local error is tightly coupled with the logic for selecting the step size and order of integration. In this experiment, the simulation is repeated with the tolerance of  $1e-2$  as well. It causes a considerable increase in the number of time steps, Jacobian, and function evaluations. Consequently, the CPU time increases with the ratio of 4:1, whereas the accuracy of simulation does not change effectively (see Figure 7.b). The norm of error between these two simulations is reported  $4.8e-3$  for phase *b*. In both tolerances, the results are practically identical to EMTP when  $\Delta t = 1 \mu s$ .

However, it should be noted that the solution methods in Modelica and EMTP are fundamentally different, and a direct comparison of variable step solver with fixed-step one is not so fair. The time steps selected in Table 1 are for demonstration/comparison purposes; in reality, it is possible to select even higher time steps without significant loss of accuracy.

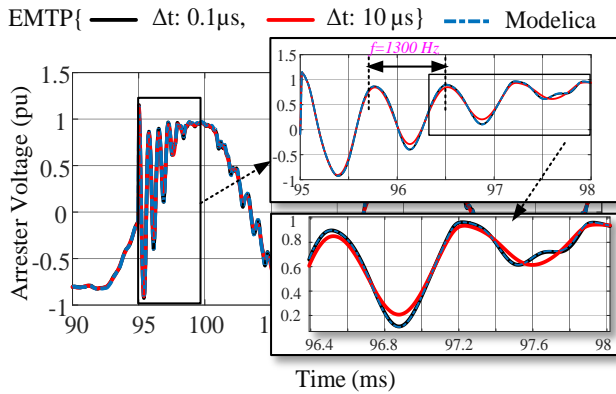


**Figure 11.** Voltage waveform of surge arrester ZnO1 on the bus SthPoint\_138\_075, DASLL solver: Tol=1e-3, EMTP solver: Trapezoidal /BE with  $\Delta t=0.1 \mu s$  and  $10 \mu s$ .

### 3.2 Case 2: Analysis of Saturation in SM

To verify the validity of the SM model in the saturation region, a large disturbance including a sudden three-phase short-circuit fault is applied at  $t = 50$  ms near to the terminals of SM “Portsmth\_Cond” and lasts till  $t = 150$  ms. The SM protective relays detect the fault and trip the generator breaker at  $t = 200$  ms. The parameters of both solvers are the same as Case 1, e.g., Tol=1e-3 in Dymola and  $\Delta t = 5 \mu s$  in EMTP.

Figure 9.a shows the phase-*a* stator voltage waveforms of the SM with and without magnetic saturation. As one can see, the results obtained from Modelica model are superimposed on EMTP ones. As time elapses, the difference between the results obtained by saturated and unsaturated models is more distinguishable on the voltage curves.

Figure 9.b depicts the field current curves of the SM with and without magnetic saturation. It is observed that the inclusion of saturation has an important impact on the excitation current needed for the generator operation.

Figure 10 illustrates the phase-*a* stator current graphs. As one can see, Modelica model yields precisely the same results as EMTP for both cases (with and without saturation). The stator current considering magnetic saturation is lower than without saturation. It is seen that the effect of saturation on the current in the sub-transient state is more than the transient state and the difference decreases as time elapses.

### 3.3 Case 3: Lightning

In this case, it is assumed that a lightning strike with the characteristics of 10kA, 8/20  $\mu s$  (see Appendix, equation (22) for the impulse source model) hits the phase-*a* of “Line\_70\_75” when the network is in steady state at  $t = 95$  ms. The surge arresters (see Appendix, Table 3 for the parameters) are located on the bus “SthPoint\_138\_075”, the nearest place to the high-voltage side of the transformer “LoadTransfo75” to protect it from transient overvoltages (see Figure 6.b). The simulation is run for 130 ms with the step sizes of 0.1  $\mu s$  (depicted by black

curve) and 10  $\mu s$  (depicted by red curve) in EMTP. Other solvers parameters are like Case 1.

Figure 11 shows the phase-*a* voltage waveforms of the arrester ZnO1. As one can see the results obtained from Modelica arrester model are identical to EMTP when  $\Delta t = 0.1 \mu s$ . A high frequency transient (1300 Hz) is created due to the strike of lightning.

Table 2 compares the performances of simulations in both tools. In Dymola, simulation is accomplished with 51513 steps in 87.2 s, which yields 1.69 ms for each time step. In this case, Dymola outperforms EMTP’s best result, that is when  $\Delta t = 0.1 \mu s$ , with the ratio of 5.56:1.

This test case is designed to show the potential advantages of variable time step solvers over fixed time step ones (like EMTP). It is designed on the purpose to illustrate the fact that a very small time step used for the short duration of the very high transient has a penalizing effect on EMTP, but not on Modelica solver. Modelica integrator expectedly reverts to a very small time step only for a short duration. It would have been possible to apply lightning in EMTP at simulation time  $t = 0$  s, and in which case the performance results would have been much better, nevertheless, our demonstration remains valid. A more practical example is the breaker arc model that also forces the usage of very small time steps and may be triggered at any point of time. It will effectively give an advantage to Modelica since in this case, it is required to capture longer simulation periods.

**Table 2.** Case 3: comparison of simulation performance.

Characteristics	Dymola	EMTP	
Solver	DASSL	Trapezoidal /BE	
Tolerance	1e-3		
$\Delta t_{MIN}$	0.623 ps	$\Delta t: 0.1 \mu s$	$\Delta t: 10 \mu s$
$\Delta t_{MAX}$	5.56 $\mu s$		
No result points	51514	1335308	21637
No accepted steps	51513	Not applicable	
f-evaluations	105576	Not applicable	
J-evaluations	1503	Not applicable	
CPU time (s)	87.2	485.6	9.9
CPU-time for 1 accepted steps	1.69 ms	0.36 ms	0.45 ms
Performance ratio	1	0.179	8.8

## Conclusion

In this paper, Modelica programming language has been considered for EMT simulations due to its advantages for creating models at very high abstraction levels. In this paper, we have emphasized the modeling of synchronous machine including magnetic saturation and surge arrester. These two nonlinear models are validated by comparisons with EMTP in a large grid (IEEE 118-bus benchmark). It is shown that high-level modeling in Modelica is very accurate as compared to EMTP. However, the performance is not satisfactory, except when variable time step is used advantageously for very high-frequency transients of short duration in a long simulation interval. Nonetheless, in comparison with Simscape Electrical SPS package, the Modelica package demonstrates an excellent



performance in the EMT simulation of large-scale networks composed of many nonlinearities.

The EMT-type package created by Modelica code is user-friendly, modular, easily expandable, and modifiable. It can be used for didactic purposes as well. Furthermore, the EMT-type models can be used for model exchange and co-simulation incorporating FMI.

This paper presents useful and practical information on currently available capabilities with Modelica for EMT simulation of large-scale grids. Future work will be oriented toward performance improvements and the inclusion of new models.

## Acknowledgments

We would like to acknowledge the continuous support of the R&D team of RTE in this research.

## Appendix

Lightning is represented by an impulse current source given by:

$$i(t) = i_m [e^{\alpha t} - e^{\beta t}] \quad (22)$$

where  $i_m = 24.9$  [kA],  $\alpha = -55$  [1/s] and  $\beta = -175$  [1/s].

**Table 3.** Exponential segments before flashover for ZnO1.

Multiplier $p$	Exponent $q$	$V_{min}$ (pu)
0.163113059479073E+02	0.240279296219978E+02	0.667857269772541E+00
0.134112947529269E+02	0.266219333383985E+02	0.107838745800672E+01
0.383838137212802E+02	0.200870413085749E+02	0.117458089341624E+01
0.115443146532003E+01	0.352906710089203E+02	0.125919561101624E+01
0.407093229412981E+03	0.111310570543275E+02	0.127478619617635E+01
0.256681175704043E+04	0.536270125014350E+01	0.137605475880033E+01

## References

- Bartolini, A., Casella, F., & Guironnet, A. (2019). "Towards pan-European power grid modelling in Modelica: Design principles and a prototype for a reference power system library". In *13th International Modelica Conference*, vol. 157, pp. 627-636. Linköping University Electronic Press.
- Braun, W., Casella, F., & Bachmann, B. (2017). "Solving large-scale Modelica models: new approaches and experimental results using OpenModelica". In *12 International Modelica Conference* pp. 557-563. Linköping University Electronic Press. DOI: 10.3384/ecp17132557.
- Fritzson, Peter (2014). *Principles of object-oriented modeling and simulation with Modelica 3.3: a cyber-physical approach*. John Wiley & Sons.
- Fritzson, P. et al. (2020), "The OpenModelica Integrated Environment for Modeling, Simulation, and Model-Based Development". *Modeling, Identification and Control*, vol. 41, no. 4, pp. 241–295, 2020. DOI: 10.4173/mic.2020.4.1.
- Guironnet, A. et al. (2018), "Towards an Open-Source Solution using Modelica for Time-Domain Simulation of Power Systems". In: *2018 IEEE PES Innovative Smart Grid Technologies Conference Europe (ISGT-Europe)*, pp. 1–6.
- Haddadi, A., & Mahseredjian, J. (2018). Power system test cases for EMT-type simulation studies. *CIGRE, Paris, France, Tech. Rep. CIGRE WG C, 4*, 1-142.
- Henningsson, E., Olsson, H., & Vanfretti, L. (2019). "DAE solvers for large-scale hybrid models." In *Proceedings of the 13th International Modelica Conference, Regensburg, Germany, March 4–6, 2019*, No. 157. Linköping University Electronic Press. DOI: 10.3384/ecp19157491
- Kocar, I. and J. Mahseredjian (2016). "Accurate Frequency Dependent Cable Model for Electromagnetic Transients". In: *IEEE Transactions on Power Delivery* 31.3, pp. 1281–1288. DOI: 10.1109/TPWRD.2015.2453335.
- Kofman, Ernesto, Joaquín Fernández, and Denise Marzorati (2021). "Compact sparse symbolic Jacobian computation in large systems of ODEs". In: *Applied Mathematics and Computation* 403, p. 126181. DOI: 10.1016/j.amc.2021.12618.
- Karaagac, U., Mahseredjian, J., & Saad, O. (2011). "An efficient synchronous machine model for electromagnetic transients". In *IEEE transactions on power delivery*, 26(4), 2456-2465. DOI: 10.1109/TPWRD.2011.2159249.
- Karaagac, U., Mahseredjian, J. and Martinez-Velasco, J. A. (2017). "Synchronous machines," in Chapter for Book "Power System Transients: Parameter Determination. Boca Raton, FL: CRC, 2009, ch. 5, pp.103–103.
- Larsson, M. (2004). "ObjectStab-an educational tool for power system stability studies". In: *IEEE Transactions on Power Systems*, vol. 19, no. 1, pp. 56-63, Feb. 2004. DOI: 10.1109/TPWRS.2003.821001
- Lemaitre, C. and P. Panciatici (2014). "iTesla: Innovative tools for electrical system security within large areas". In: *2014 IEEE PES General Meeting Conference Exposition*, pp. 1–2. DOI: 10.1109/PESGM.2014.6939447.
- Mahseredjian, J., S. Denetière, et al. (2007). "On a new approach for the simulation of transients in power systems". In: *Electric Power Systems Research* 77.11. Selected Topics in Power System Transients - Part II, pp. 1514–1520. ISSN: 0378-7796. DOI: 10.1016/j.epsr.2006.08.027.
- Mahseredjian, J., V. Dinavahi, and J. A. Martinez (2009). "Simulation Tools for Electromagnetic Transients in Power Systems: Overview and Challenges". In: *IEEE Transactions on Power Delivery* 24.3, pp. 1657–1669. DOI: 10.1109/TPWRD.2008.2008480.
- Masoom, Alireza et al. (2020). "Simulation of electromagnetic transients with Modelica, accuracy and performance assessment for transmission line models". In: *Electric Power Systems Research* 189, p. 106799. DOI: 10.1016/j.epsr.2020.106799.
- Masoom, Alireza et al. (2021). "Modelica-based Simulation of Electromagnetic Transients Using Dynawo: Current Status and Perspectives". In: *Electric Power Systems Research* 197, 107340. DOI: 10.1016/j.epsr.2021.107340.
- Petzold, L. R. (1982). *Description of DASSL: a differential/algebraic system solver* (No. SAND-82-8637; CONF-820810-21). Sandia National Labs., Livermore, CA (USA).
- Sana, A. R., Mahseredjian, J. et al. (1995). "Treatment of discontinuities in time-domain simulation of switched networks". In *Mathematics and Computers in Simulation*, vol. 38, pp. 377-387. DOI: 10.1016/0378-4754(95)00047-2.
- Simscape Electrical (2020), Specialized Power Systems User's Guide Release 2020b, Hydro-Quebec and Math Works, Sep. 2020.
- Vanfretti, L., Rabuzin, T., Baudette, M., & Murad, M. (2016). "iTesla Power Systems Library (iPSL): A Modelica library for phasor time-domain simulations". In: *SoftwareX*, vol: 5, pp. 84-88. DOI: 10.1016/j.softx.2016.05.001.